

Implementation and Critical Investigation on Modulation Schemes of Three Phase Impedance Source Inverter

S. Thangaprakash* and A. Krishnan**

Abstract: New control circuits and algorithms are frequently proposed to control the impedance (Z) source inverter in efficient way with added benefits. As a result, several modified control techniques have been proposed in recent years. Although these techniques are clearly superior to the simple boost control method which was initially proposed along with the Z-source inverter (ZSI), little or conflicting data is available about their merits relating to each other. In this paper, it is shown how the shoot-through periods are inserted in the switching waveforms of the power switches and the performances of them are analyzed based on the operation of ZSI. Simple boost control, maximum boost control, constant boost control and space vector modulation based control methods given in the literature has been illustrated with their control characteristics. A critical investigation on ripples of the impedance source elements, output voltage controllability, output harmonic profile, transient response of the voltage across the impedance source capacitor and voltage stress ratio etc has been presented with the simulation results. The simulation results are experimentally verified in the laboratory with digital signal processors (DSP). DSP coding for the above all control techniques has been generated by interfacing Matlab/Simulink with DSP C6000 tool box and signal processing block set.

Keywords: Z-source inverter, simple boost control, maximum boost control, constant boost control, space vector modulation; buck-Boost.

1 Introduction

With the introduction and wide acceptance of ZSI (shown in Fig. 1) as an alternative for traditional voltage source and current source inverters (VSI/CSI), the modified switching schemes from the traditional schemes has reached the point where the further improvements in firing the switches and inserting the shoot-through states bring crucial benefits. In addition to the six active switching states of the VSI, a ZSI has seven shoot-through zero states, when the positive and negative switches of a same phase leg are simultaneously switched on. This shoot-through state is harmful in VSI/CSI and can result short circuiting and damaging of entire application. Due to the capability of buck-boost and wide range of operating points, ZSIs are suitable for the applications with unstable power supply such as fuel cell, wind power, photovoltaic etc. Same pulse width modulation (PWM) logics and methods of

VSIs can be adapted to switch a ZSI with slight modifications. The distribution of the shoot-through in the switching waveforms of the traditional PWM concept is the key factor to control the ZSI. The dc link voltage boost (diagonal capacitor voltage), controllable range of ac output voltage, voltage stress across the switching devices and harmonic profile of the ac output parameters are purely based on the method of control algorithm adapted to insert the shoot-through. There are number of control methods have been presented in recent years that include sinusoidal pulse width modulation (SPWM) and modified space vector modulation based pulse width modulation (SVPWM) techniques. In this paper, the implementation logics of PWM control algorithms: simple boost control (SBC), maximum boost control (MBC), constant boost control (CBC), and traditional and modified space vector based pulse width modulation schemes (TSVM & MSVM) are elaborated and their performance/control characteristics are investigated in many fonts.

SBC with constant boost factor was proposed by Peng [1], it uses two straight lines equal to or greater than the peak value of the three phase references to control the shoot-through duty ratio in a traditional SPWM. In MBC, under a given modulation index and shoot-through duty ratio, a maximum boost in the dc link

Iranian Journal of Electrical & Electronics Engineering, 2010.

Paper first received 21 Dec. 2010 and in revised form 14 Apr. 2010.

* The Author is with the Department of Electrical and Electronics Engineering, Sri Shakthi Institute of Engineering and Technology, Coimbatore, India.

E-mail: s_thangaprakash@rediffmail.com.

** The Author is Dean (Academic), K.S.R College of Engineering, Tamil Nadu, India.

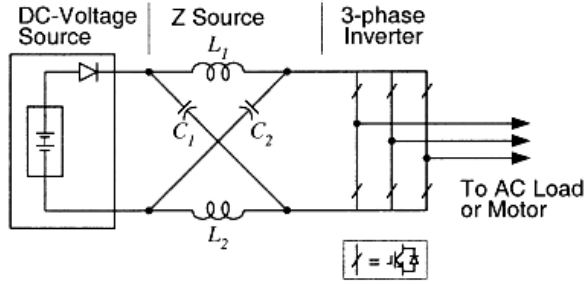


Fig. 1 Three phase impedance source inverter topology

voltage than SBC is achievable to produce the maximum voltage gain [2]. CBC provides a maximum voltage gain at any given modulation index without producing any low-frequency ripple that is related to the output frequency [3].

TSVM for ZSI is discussed in [4] about how various conventional PWM strategies can be modified to switch a ZSI either continuously or discontinuously, while retaining all the unique harmonic performance features. Several modified modulation techniques to control ZSI are frequently reported by various researchers. An indirect controller for the dc-link voltage on the dc side of the ZSI along with AC voltage control with MSVM was discussed in [5]. MSVM with maximum boost in the dc link voltage along with better output harmonic profile and its application to induction motor drive has been discussed by Thangaprakash & Krishnan [6-8]. Modeling and control of fuel cell based ZSI has been presented in [9] and the same for induction motor drives have been discussed in [10].

In this paper the control methods presented in [1-5] are investigated with their control characteristics and performances. The implementation logics and important expressions of all the control methods are briefed in the next section followed by the simulation results and their discussion. The Acronyms are as follows:

| | |
|-------------------|------------------------------|
| \hat{v}_{ac} : | Peak Value of the AC voltage |
| T_s : | Switching Period |
| T_0 : | Shoot-through Time Period |
| T_z : | Traditional Zero Period |
| v_i : | DC Link Voltage |
| m_a : | Modulation Index |
| D_0 : | Shoot-through Duty Ratio |
| B : | Boost Factor |
| G : | Voltage Gain |
| $V_{dc} \& V_0$: | DC Supply Voltage |
| V_s : | Voltage Stress |

2 Pulse Width Modulation Schemes

The basic idea to control the ZSI is to turn traditional zero state into shoot-through zero state, while keeping the active vectors unchanged, thus we can maintain the sinusoidal output and at the same time

achieve voltage boost from the shoot-through of the dc link.

2.1 Simple Boost Control

In SBC, the shoot-through periods are fabricated by two straight lines which are equal or greater than the (maximum and minimum) peak values of the modulating reference sinusoidal signals. Fig. 3 shows the complete implementation block diagram of the SBC technique. Shoot-through switching pulses are generated by comparing the dc signal (with magnitude equal or greater than the peak of triangular signal) with the high frequency triangular carrier signal. To produce switching pulses, three phase reference wave forms having peak value with modulation index (m_a) are compared with the same high frequency triangular signal. Comparator compares these two signals and produces pulses (when $V_{sin} > V_{tri}$, on and $V_{sin} < V_{tri}$, off). Shoot-through pulses are inserted in to the switching waveforms by logical OR gate. These pulses are then sent to gates of the power IGBT's through isolation and gate drive circuit.

Major expressions of SBC method are outlined here,

$$G = \frac{\hat{v}_{ac}}{v_i} = m_a * B = \frac{m_a}{1 - 2D_0} = \frac{m_a}{2m_a - 1} \quad (1)$$

$$m_a = \frac{G}{2G - 1} \quad (2)$$

$$V_s = B * V_0 = (2G - 1) * V_0 \quad (3)$$

$$\frac{V_s}{G * V_0} = 2 - \frac{1}{G} \quad (4)$$

The voltage stress across the switches is quite high when SBC is used, this characteristic will restrict the obtainable voltage gain because of the limitation of device voltage rating [2].

2.2 Maximum Boost Control

Reducing the voltage stress under a desired voltage gain now becomes important to the control of ZSI. MBC turns all traditional zero states into shoot-through zero state. The implementation block diagram of the MBC is shown in Fig. 3. MBC maintains the six active states unchanged and turns all zero states into shoot-through zero states. Thus maximum T_0 and B are obtained for any given modulation index without distorting the output waveform. As can be seen from Fig. 3, the circuit is in shoot-through state when the triangular wave is either greater than the maximum curve of the references (V_a, V_b and V_c) or smaller than the minimum of the references. The shoot-through duty cycle varies each cycle. Low frequency current ripples associated with the output frequency are introduced in inductor current and capacitor voltage waveform [3].

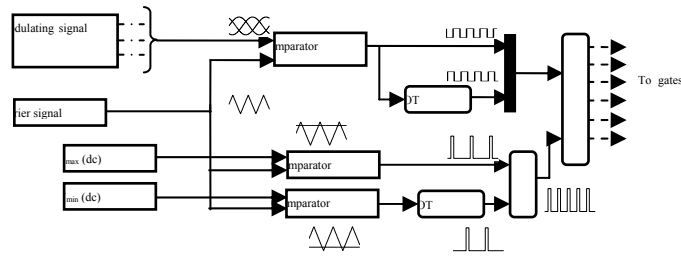


Fig. 2 Implementation block diagram of simple boost control.

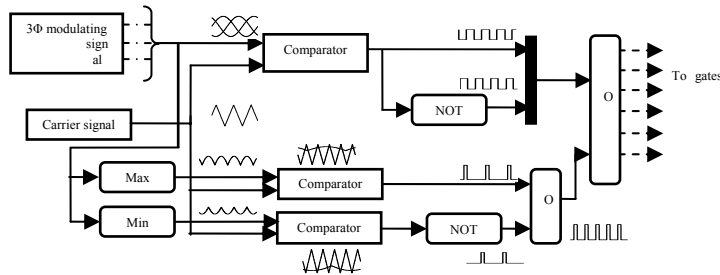


Fig. 3 Implementation block diagram of MBC.

The shoot-through state repeats periodically every $(\pi/3)$. Assume that the switching frequency is much higher than the modulation frequency; the average shoot-through duty ratio over one switching cycle in the interval $(\pi/6, \pi/2)$ can be expressed as

$$\begin{aligned} \frac{\hat{T}_0}{T} &= \frac{\int_{\pi/6}^{\pi/2} (2 - m_a \sin \theta - m_a \sin(\theta - 2\pi/3))}{2} \\ &= \frac{2\pi - 3\sqrt{3}\pi}{2\pi} \end{aligned} \quad (5)$$

Maximum shoot-through duty ratio can be written as,

$$D_0 = \frac{2\pi - 3\sqrt{3}\pi}{2\pi} \quad (6)$$

Major expressions of SBC method are outlined here,

$$G = \frac{m_a}{1 - 2D_0} = \frac{m_a \pi}{3\sqrt{3}m_a - \pi} \quad (7)$$

$$m_a = \frac{\pi G}{3\sqrt{3}G - \pi} \quad (8)$$

$$B = \frac{3\sqrt{3}G - \pi}{\pi} \quad (9)$$

$$V_s = B * V_{dc} = \frac{3\sqrt{3}G - \pi}{\pi} V_{dc} = \frac{\pi}{3\sqrt{3}G - \pi} V_{dc} \quad (10)$$

$$\frac{V_s}{G * V_0} = \frac{3\sqrt{3}}{\pi} - \frac{1}{G} \quad (11)$$

2.3 Constant Boost Control

In order to reduce the volume and cost, it is important always to keep the shoot-through duty ratio constant. At the same time, a greater voltage boost for any given modulation index is desired to reduce the voltage stress across the switches. Implementation block diagram of CBC is shown in Fig. 4 with such feature. There are five modulation curves in this control method: three reference signals, V_a , V_b , and V_c , and two shoot-through envelope signals, V_p and V_n . When the carrier triangle wave is greater than the upper shoot-through envelope, V_p , or lower than the lower shoot-through envelope, V_n , the inverter is turned to a shoot-through zero state. In between, the inverter switches in the same way as in traditional carrier-based PWM control. CBC achieves maximum boost while keeping the shoot-through duty ratio always constant; thus it results in no line frequency current ripple through the inductors. With this method, the inverter can buck and boost the voltage from zero to any desired value smoothly within the limit of the device voltage.

Major expressions of CBC method are outlined here,

$$D_0 = \frac{2 - \sqrt{3}m_a}{2} = 1 - \frac{\sqrt{3}m_a}{2} \quad (12)$$

$$B = \frac{1}{1 - 2\frac{T_0}{T}} = \frac{1}{\sqrt{3}m_a - 1} \quad (13)$$

$$\frac{\hat{v}_i}{V_{dc}/2} = m_a * B = \frac{m_a}{\sqrt{3}m_a - 1} \quad (14)$$

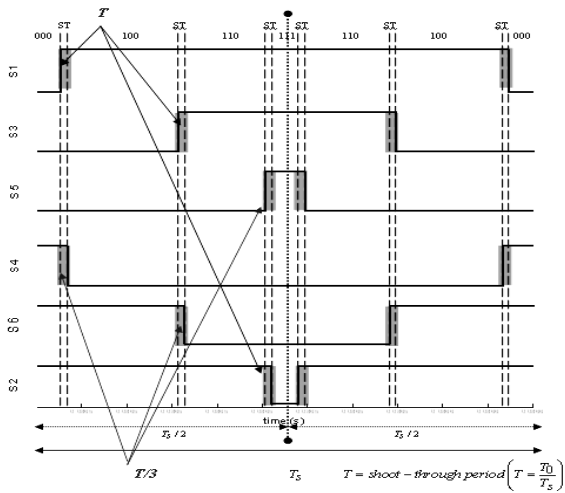


Fig.4 Implementation block diagram of CBC.

$$G = m_a * B = \frac{m_a}{\sqrt{3}m_a - 1} \quad (15)$$

$$m_a = \frac{G}{\sqrt{3}G - 1} \quad (16)$$

$$V_s = B * V_{dc} = (\sqrt{3}G - 1)V_{dc} \quad (17)$$

$$\frac{V_s}{G * V_0} = \sqrt{3} - \frac{1}{G} \quad (18)$$

By using CBC, the ZSI can achieve the minimum passive component requirements. Although this method will increase the voltage stress across the devices by a small amount compared to the MBC, this method is very suitable for minimizing the impedance source network, especially in low frequency or variable speed drive applications.

2.4 Traditional Space Vector PWM

The continuous centered SVM state sequence of a conventional three phase VSI, where three state transitions occur (e.g., null (000) → active(100) → active (110) → null (111)) and the null states are placed at the start and end of a switching cycle T_s span equal time intervals to achieve optimal harmonic performance. The switching waveforms for the sector 1 of the voltage space vector are shown in Fig. 5. With three-state transitions, three equal-interval ($\frac{T_0}{6}$) shoot-through states can be added immediately adjacent to the active states per switching cycle for modulating a ZSI where T_0 is the shoot-through time period in one switching cycle.

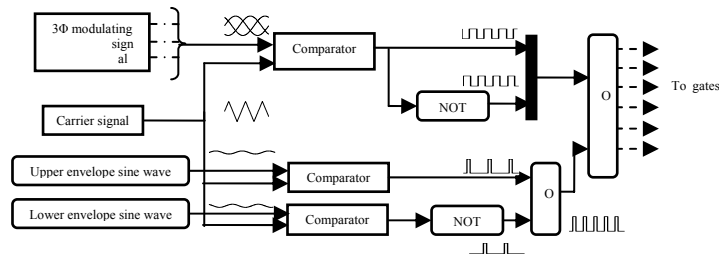


Fig. 5 Switching pulse pattern for sector 1 using TSVM.

Preferably, the shoot-through states should be inserted such that equal null intervals are again maintained at the start and end of the switching cycle to achieve the same optimal harmonic performance. The middle shoot-through state is symmetrically placed about the original switching instant. The active states {100} and {110} are left/right shifted accordingly by ($T_0/6$) with their time intervals kept constant, and the remaining two shoot-through states are lastly inserted within the null intervals, immediately adjacent to the left of the first state transition and to the right of the second transition.

Major expressions of TSVM are outlined here,

$$D_0 = \frac{3}{4} * \frac{2\pi - 3\sqrt{3}m_a}{2\pi} \quad (19)$$

$$B = \frac{4\pi}{9\sqrt{3}m_a - 2\pi} \quad (20)$$

$$G = \frac{\hat{v}_i}{V_{dc}/2} = \frac{4\pi m_a}{9\sqrt{3}m_a - 2\pi} \quad (21)$$

$$V_s = \frac{9\sqrt{3}G - 4\pi}{2\pi} V_{dc} \quad (22)$$

$$\frac{V_s}{G * V_0} = \frac{9\sqrt{3}}{2\pi} - \frac{2}{G} \quad (23)$$

2.5 Modified Space Vector PWM

In MSVM, the shoot-through states are evenly assigned to each phase with ($T_{sh}/6$) within zero voltage period T_0 , as shown in Fig. 6. The zero voltage periods should be diminished for generating a shoot-through time, and the active states T_1 and T_2 are unchanged. So, the shoot-through time does not affect the PWM control of the inverter, and it is limited to the zero state time. The six PWM signals in the MSVM scheme should be controlled independently.

In order to overcome the non-linear characteristics of capacitor voltage and shoot-through, the algorithm for controlling linearly the capacitor voltage is proposed [5]. This algorithm is shown in Fig. 7. The output of the PI controller of V_C becomes K and can be defined as,

$$K = \frac{V_c}{V_0} \quad (24)$$

where the K is greater than 1 for stepping up the capacitor voltage.

Major expressions of MSVM method are outlined here,

$$T_0 = \frac{K-1}{2K-1} T_s \quad (25)$$

$$B = \frac{1}{1-2D_0} = \frac{\pi}{3\sqrt{3}m_a - \pi} \quad (26)$$

$$G = \frac{\hat{v}_i}{V_{dc}/2} = \frac{4\pi m_a}{7\sqrt{3}m_a - \pi} \quad (27)$$

$$V_s = \frac{3\sqrt{3}G - \pi}{\pi} V_{dc} \quad (28)$$

$$\frac{V_s}{G*V_0} = \frac{19\sqrt{3}}{4\pi} - \frac{2}{G} \quad (29)$$

3 Results and Discussions

For the same system parameters and operating points the performance of the Z-source inverter under all the above control methods has been conducted to observe the characteristics of the control methods. The relative results are analyzed for different control variables and are shown in this section. For each method, the boost factor, voltage gain, duty ration and voltage stress across the switches are expressed and the relationships among them are analyzed in detail. Table 1 shows the system parameters used for Matlab/Simulink.

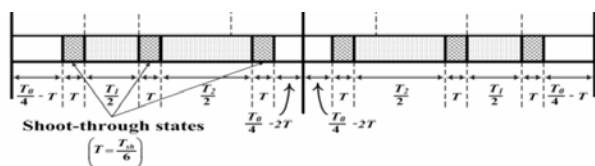


Fig. 6 Switching pattern for sector-I using MSVM.

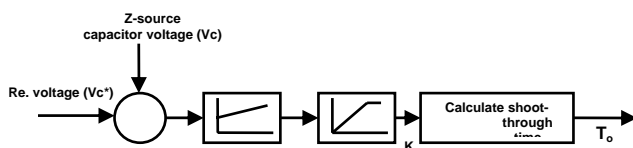


Fig. 7 Linearization of capacitor voltage.

Table 1 System parameters.

| Parameter | Specification |
|---------------------|---------------|
| DC Supply | 150 V |
| Modulation index | 0.8 |
| Output frequency | 50 Hz |
| Switching frequency | 5000 Hz |
| Shoot through | 0.2 |
| $C_1=C_2=C$ | 1000 μ F |
| $L_1=L_2=L$ | 1 mH |
| R_{Load} | 10 Ohms |
| L_{Load} | 5 mH |

3.1 Simulation Results

To investigate the characteristics of different PWM control techniques discussed in this paper, simulations and experiments were conducted. The simulation results are presented in this section and the relevant waveforms are given. Fig. 8 shows the simulation results of SBC, MBC and CBC for the system parameters shown in Table 1. In SBC method, the shoot-through time per switching cycle is kept constant, thus having a constant boost factor. As a result, the dc inductor current and capacitor voltage have no ripples that are associated with the output frequency. MBC produces the maximum voltage boost under a given modulation index than the other control methods. CBC does not introduce any extra harmonic contents compared to the traditional VSI with the same modulation index and same output voltage. Voltage stress in the MBC is much lower than the SBC, which means that for given devices, the inverter can be operated to obtain a higher voltage gain. In CBC the voltage stress is still lower than the MBC.

Fig. 9 shows the simulation results of TSVM and MSVM based approaches. In the MSVM, the transient responses of the dc capacitor voltage of the ZSI can be improved by controlling linearly the capacitor voltage. The peak ac output voltage was used to control exactly the ac output voltage to its desired level. The MSVM method can achieve the good transient responses of variations of both the reference capacitor voltage and the reference output voltage. For the same operating environment, the MSVM provide better voltage boost and better output voltage control over TSVM.

3.2 Relative Investigation

This section investigates the performance comparison of all control methods with same operating points. The voltage boost is inversely related to the shoot-through duty ratio; therefore, the ripple in shoot-through duty ratio will result in ripple in the current through the inductor, as well as in the voltage across the capacitor. Table 2 shows the ripple profile of Z-source elements for different values of shoot-through duty ratio. As already discussed, the SBC has less ripples in voltage across the capacitors and current through the inductors than all other methods. It is observed that, the ripple factor increases while increasing the shoot-through time periods. In the space vector based control methods, the MSVM provides fewer ripples than the TSVM.

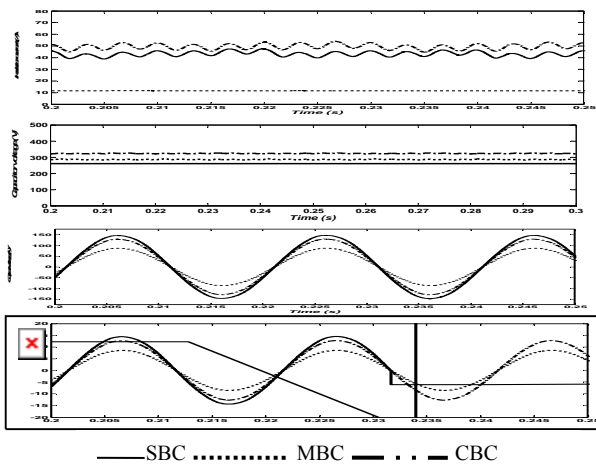


Fig. 8 Simulation results of SBC, MBC and CBC.

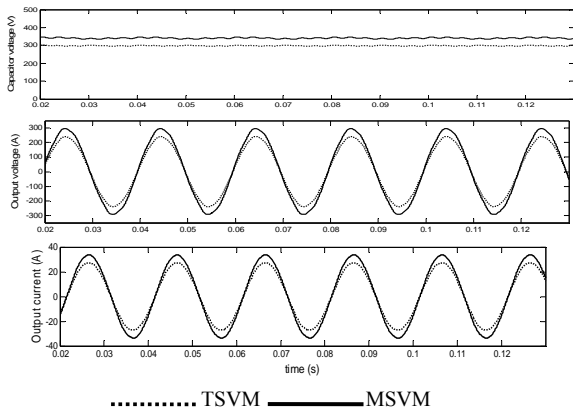


Fig. 9 Simulation results of ZSI using TSVM and MSVM.

Table 2 Profile of Z-source ripples.

| Method | Shoot-through | Z-source elements | |
|--------|---------------|---------------------|---------------------|
| | | Current ripple in L | Voltage ripple in C |
| SBC | Do=0.2 | 6 | 4 |
| | Do=0.3 | 6.23 | 4.6 |
| MBC | Do=0.2 | 10 | 5 |
| | Do=0.3 | 11.2 | 5.8 |
| CBC | Do=0.2 | 8 | 4 |
| | Do=0.3 | 9.2 | 4.8 |
| TSVM | Do=0.2 | 6 | 6 |
| | Do=0.3 | 7 | 7.1 |
| MSVM | Do=0.2 | 5.5 | 4.5 |
| | Do=0.3 | 7 | 5.3 |

The harmonic profile of the output voltage/current of ZSI for different control methods are given in Table 3. In this comparison, the SBC has fewer harmonic in the output side than the other methods. The graph between voltage gain and modulation index for all the control methods are depicted in Fig. 10. This chart shows that, the SBC has less voltage gain for lower modulation indices. MBC gives better gain for lower modulation indices and for higher modulation indices,

MSVM provides better voltage gain. CBC provides optimum voltage gain for all the operating points.

Table 3 Harmonic profile.

| Method | Shoot-through | Harmonic profile | |
|--------|---------------|--------------------|--------------------|
| | | THD _v % | THD _i % |
| SBC | Do=0.2 | 83 | 0.6 |
| | Do=0.3 | 85 | 0.6 |
| MBC | Do=0.2 | 65 | 3 |
| | Do=0.3 | 66 | 3.13 |
| CBC | Do=0.2 | 70 | 0.45 |
| | Do=0.3 | 71 | 0.5 |
| TSVM | Do=0.2 | 72 | 2.18 |
| | Do=0.3 | 75 | 2.5 |
| MSVM | Do=0.2 | 65 | 1.8 |
| | Do=0.3 | 68.5 | 1.6 |

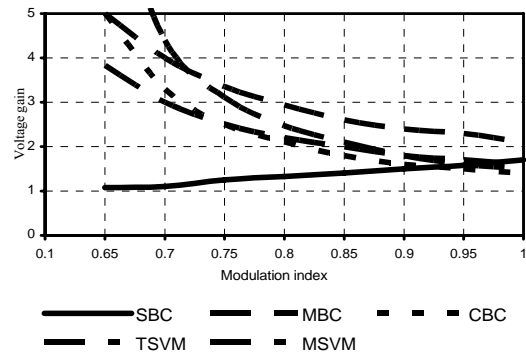


Fig. 10 Graph between voltage stress and voltage gain.

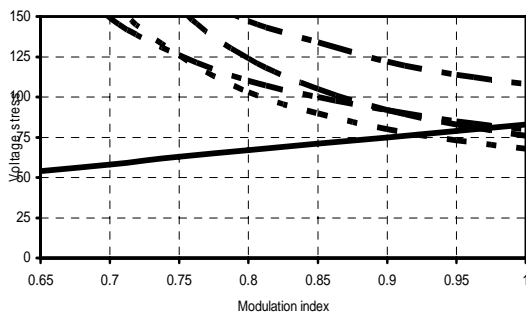


Fig. 11 Graph between voltage stress and modulation index.

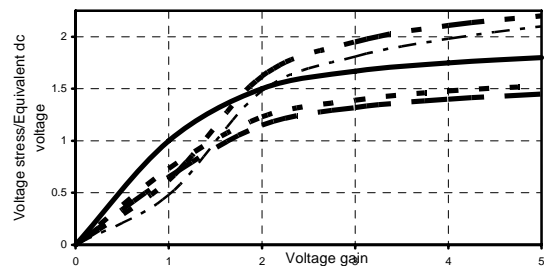


Fig. 12 Graph between shoot-through duty ratio Vs boost factor.

Fig. 11 shows the graph between voltage stress and modulation index. It is clear that, the voltage stress of the power switching devices is decreased when the modulation index is increased. The TSVM based technique provides superior operation when it is compared with all control methods. For the lower modulation indices, the MBC produces high voltage stress across the devices. Fig. 12 shows the graph between voltage stress-equivalent dc voltage ratio and voltage gain. As can be seen from Fig. 12, the CBC has a much lower voltage stress across the devices than the SBC and TSVM, while having a slightly higher voltage stress than the MSVM method. The ideal voltage-stress ratio is one. The ratio of the voltage stress to the equivalent dc voltage represents the cost that the ZSI has to pay to achieve voltage boost. The CBC is highly desirable for applications requiring a voltage gain of two to three. As we can see from the curves, only an extra 30% voltage stress is needed for CBC to achieve a voltage gain of 2.5. CBC requires the minimum inductance and capacitance because the inductor current and capacitor voltage contain no low-frequency ripples associated with the output voltage, thus reducing the cost, volume, and weight of the Z-source network. The output ac voltage for different values of modulation index for the duty ratio 0.2, for all the control methods is evidently shown in the Table 4. In SBC, MBC and CBC the shoot-through current is equally distributed on the three phases of the inverter bridge which limit the current stress on the switch. But, in TASM and MSVM, the shoot-through current for each phase is twice the inductor current, which increase the current stress on the switch. Also, in high power range the PWM strategy with six shoot-through state insertions in one switching cycle (TSVM and MSVM) brings more losses than its counterpart of two shoot-through state (SBC, MBC and CBC) insertions in one switching cycle and higher switching frequency makes the efficiency gap become larger.

The transient response of the voltage across Z-source capacitor has been shown in Figs. 13-14. SBC has less peak overshoot when it is compared with MBC and CBC. In space vector modulation based techniques, The MSVM has less peak overshoot. Hence the transient response of the overall ZSI system is superior in MSVM scheme. The MSVM can achieve the good transient responses of variations of both the reference capacitor voltage and the reference output voltage, and also during supply voltage sags.

3.3 Experimental Results

The results shown in simulation are verified by the experiment in the laboratory with ZSI. The control system is implemented by TMS320C6713 digital signal processor (DSP). The ac output voltage and current of the ZSI are sensed by isolation devices, amplifiers, and a 12-bit analog to digital converter within the DSP. The Matlab/Simulink interfaced DSP generated PWM pulses

were then sent out through six independent PWM channels to gate the six switches (IGBT modules) of the implemented inverter. The laboratory experimental setup for producing switching waveforms for different control techniques is shown in Fig. 15. Matlab/Simulink is interfaced with DSP by code composer studio, embedded target C6000 and DSP tool box.

Figs. 16-18 show the experimental results of ZSI using space vector modulation based methods. Fig. 16 shows, the placement of shoot-through state in modulating signal (encircled portion). Experimental modulation signal for phase A using TSVM and MSVM are shown in Fig. 17. The experimental switching line voltage waveform of the inverter after the LC filter with cutoff frequency 1.0 kHz for $m_a = 0.8$; $D_o = 0.2$; boost factor $B = 1.66$ for the 250 V_{dc} are shown in Fig. 18.

All the control methods described in this paper are practically implemented with DSP based control unit and their results are verified with the simulation results. Due to the page limitation, only the results of SVM techniques are presented in this paper.

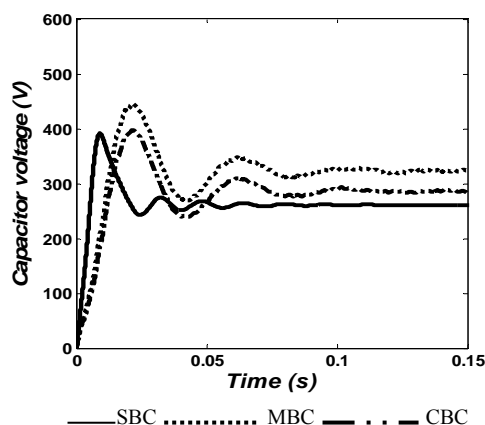


Fig. 13 Transient response of Z-source capacitor voltage by SBC, MBC and CBC.

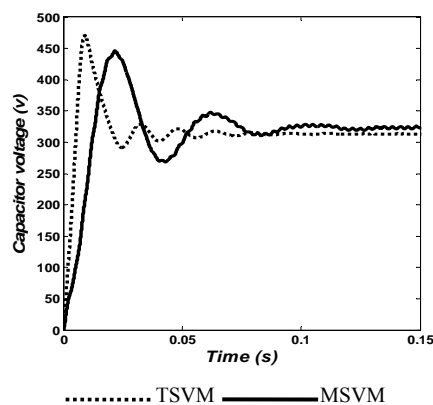


Fig. 14 Transient response of Z-source capacitor voltage by traditional SVM and Modified SVM.

Table 4 AC output voltage profile.

| m_a | SBC | MBC | CBC | TSVM | MSVM |
|-------|-------|--------|--------|--------|--------|
| 0.65 | 54.2 | 432.2 | 258.3 | 191.7 | 255.6 |
| 0.7 | 58.33 | 221.81 | 164.75 | 149.67 | 199.6 |
| 0.75 | 62.5 | 155.93 | 125.4 | 125.7 | 167.7 |
| 0.8 | 66.67 | 123.76 | 103.72 | 110.3 | 147.13 |
| 0.85 | 70.8 | 104.7 | 90 | 99.57 | 132.77 |
| 0.9 | 75 | 92.1 | 80.5 | 91.6 | 122.2 |
| 0.95 | 79.1 | 83.1 | 73.6 | 85.5 | 114 |
| 1 | 83 | 76.5 | 68.3 | 80.7 | 107.6 |

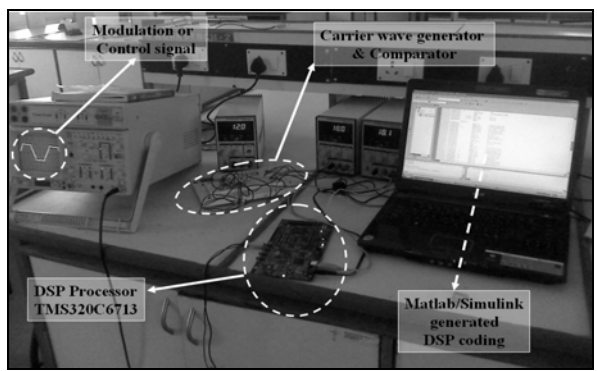


Fig. 15 Experimental setup for switching waveform generation.

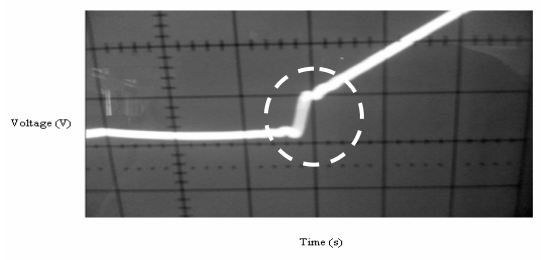


Fig. 16 Placement of shoot-through state in modulating signal.

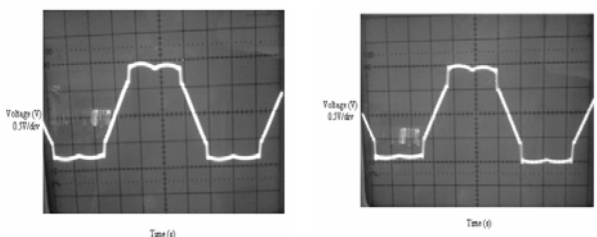


Fig. 17 Experimental modulation signals for phase A by TSVM (upper) and MSVM (lower).

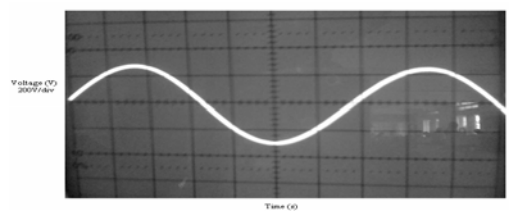


Fig. 18 Experimental switching voltage waveform for phase A in MSVM.

4 Conclusions

The critical investigation on PWM control schemes for ZSI has been presented in this paper. For the same input and system parameters the results of different control methods are analyzed. The transient response of the Z-source capacitor voltage has been discussed to describe the dynamic behavior of the inverter. Through the use of relevant theoretical and experimental results it has been shown that, for each major area of application there is a specific optimum pulse width modulation method. The experimental results obtained in the laboratory have close agreement with the simulation results.

References

- [1] Peng F. Z., "Z-source inverter", *IEEE Transactions on Industry Applications*, Vol. 39, No. 2, pp. 504-510, 2003.
- [2] Peng F. Z., Shen M. and Qian Z., "Maximum boost control of the Z-source inverter", *IEEE Transactions on Power Electronics*, Vol. 20, No. 4, pp. 833-838, 2005.
- [3] Shen M., Wang J., Joseph A. and Peng F. Z., "Constant boost control of the Z-source inverter to minimize current ripple and voltage stress", *IEEE Transactions on Industry Applications*, Vol. 42, No. 3, pp. 770-778, 2006.
- [4] Loh P. C., Vilathgamuwa M., Lai Y. S., Chua G. T. and Li Y. W., "Pulse width modulation of Z-source inverters", *IEEE Transactions on Power Electronics*, Vol. 20, No. 6, pp. 1346-1355, 2005.
- [5] Tran Q. V., Chun T. W., Ahn J.R. and Lee H. H., "Algorithms for Controlling Both the DC Boost and AC output Voltage of Z-source Inverter", *IEEE Transactions on Industrial Electronics*, Vol. 54, No. 5, pp. 2745-2750, 2007.
- [6] Thangaprakash S. and Krishnan A., "An integrated control algorithm for an effective control of Z-source inverter using modified voltage space vector", *Australian Journal of Electrical and Electronics Engineering*, Vol. 7, No 1, pp. 53-64, 2010.
- [7] Thangaprakash S. and Krishnan A., "Performance improvement of Z-source inverter fed induction motor drives using modified voltage space

vector”, *Australian Journal of Electrical and Electronics Engineering*, Online, pp. 59-70, 2010.

- [8] Thangaprakash S. and Krishnan A., “Current mode integrated control technique for Z-source inverter fed induction motor drives”, *Journal of Power Electronics*, Vol. 10, No. 3, pp. 1-8, 2010.
- [9] Wang J. W. and Keyhani A., “Control of a fuel cell based Z-source converter”, *IEEE Transactions on Energy Conversion*, Vol. 22, No. 2, pp. 467-476, 2007.
- [10] Peng F. Z., Yuwan X., Fang X. and Qian Z., “Z-source inverter for motor drives”, *IEEE Transactions on Power Electronics*, Vol. 20, No. 4, pp. 857-863, 2005.
- [11] Holtz J., “Pulse width modulation - a survey”, *IEEE Transactions on Industrial Electronics*, Vol. 39, No. 5, pp. 410-420, 1992.



Sengodan Thangaprakash received his Bachelor of Engineering in Electrical and Electronics Engineering from Kongu Engineering College, Bharathiar University, Tamil Nadu, India in 2002 and his Master of Engineering in Power Electronics and Drives from the Government College of Technology,

Tamilnadu, India in 2004. Presently he is affiliated with the Department of Electrical and Electronics Engineering in the Sri Shakthi Institute of Engineering and Technology, Coimbatore, India. Currently he is working towards his PhD degree at Anna University, Chennai, India. His research interests include power electronics circuits, renewable power conversion systems and solid state control of electrical drives. He has published more than twenty papers in international journals and conferences. He is a life member of Indian Society of Technical Education (ISTE).



Ammasai Krishnan received his Bachelor of Engineering in Electrical Engineering and his Master of Engineering in Control Systems from Madras University, India in 1966 and 1974 respectively. Then he received his PhD in Electrical Engineering (Control & Computers group) from the Indian

Institute of Technology, Kanpur in 1979. He has been in the field of technical teaching and research for more than four decades at the Government College of Technology and the Coimbatore Institute of Technology, Coimbatore, India. From 1994 to 1997, he was an Associate Professor in Electrical Engineering at the University Pertanian Malaysia (UPM), Malaysia. Currently he is a Dean of the K.S.R. College of Engineering, Tamil Nadu, India. His research interests include control systems, power electronics and electrical machines. He has published more than 180 papers in international journals and conferences. He is a senior member of IEEE.